JPMTR-2303
DOI 10.14622/JPMTR-2303
UDC 681.6|53.088(182)

Review paper | 180
Received: 2023-02-21
Accepted: 2023-07-04

Two-dimensional register error

Günther Brandenburg

Tölzer Str. 41, 82194 Gröbenzell gap.brandenburg@t-online.de

Abstract

On contemporary web printing machines, longitudinal and lateral register control of high precision is a crucial requirement for successful use in the roll-to-roll production of multi-layer electronic components. In the present study, an overview of mathematical models of two-dimensional register errors is shown. Simulation of the register errors is enabled by the use of a multi-layer model. Representation of the influencing variables on the lateral and longitudinal register errors and the mass flow chain is given in a joint block diagram that can be further used for simulation purposes.

Keywords: block diagram, moving web, mass flow, transfer function, web deflection

1. Introduction

In the development of rotary presses, two lines of development can be identified. The first line is very fast-running machines. These must have only very small longitudinal register errors and must not show doubling under any circumstances (Brandenburg, 2000). The lateral register errors, however, are of secondary importance. These requirements were met by each printing unit being driven by a single drive that is digitally controlled. Numerous tests and simulations were necessary to master such a system with "electronic shaft" in practice (Brandenburg, et al., 1999). The simulations required mathematical models of the moving web and the individual electric drives. These tools only became available after the development of powerful computers. The second line of development is much newer. This involves the production of multi-layer printed circuit boards for later assembly with electronic components. In addition to the longitudinal register error, the lateral register error is also of utmost importance for these slow-running machines. The lateral register error must be smaller by a factor of 10 than for the former machines. The moving elastic web can be represented by the well-known mathematical model of the so-called mass flow (Kang 2010; Kang, Lee and Shin, 2011).

1.1 State of the art

The treatment of the register error in the longitudinal direction of the web, the so-called longitudinal register error, has been completed theoretically and to a large extent experimentally, as exemplified by the publications of Brandenburg (1976a; 1976b; 1976c; 2011; 2015), Brandenburg and Tröndle (1976a; 1976b), and Tröndle (1973).

Concerning the lateral register error, H. K. Kang has made a comprehensive contribution (Kang, 2010; Kang, Lee and Shin, 2011). He has investigated a rotogravure press that can be used to produce printed circuits "from roll to roll." He developed a mathematical model of lateral register error and verified it experimentally, showed the coupling between longitudinal and lateral register error, and investigated numerous variants for controls.

In the present paper, however, the model from Brandenburg and Klemm (2019) is used, which was originally derived only for constant web velocity. This is extended by linearization to variable web velocities. From this, a calculation rule for the lateral register error is derived for the first time. Further theory is restricted to a Bernoulli web, i.e. narrow webs with the ratio $L/b \geq 10$ (with the length L and the width b). For these, it can be shown that the web equations for lateral motion and those for mass flow (continuity equation) are only slightly coupled. Furthermore, it can be stated that there is hardly any difference between the continuity equation in longitudinal transport direction x, and in lateral transport direction, y. This makes it possible for the first time to represent the lateral and longitudinal register errors with the longitudinal mass

flow equations in a joint block diagram, thus providing a comprehensive plan of the system for simulation purposes.

2. Lateral register error at constant web speed

Let the three-roller system with rollers 1, 2, and 3 as shown in Figure 1 be given. These are three printing units that are in synchronism and print three colors or layers on a substrate congruently on top of each other. The travelling web is a Bernoulli web and is at first assumed to be transported at the constant web speed v. It is assumed at roller 1 that the web experiences an input disturbance in the form of an input displacement $y_{E1}(t)$ or/and a change in the input angle $\theta_{E1}(t)$.

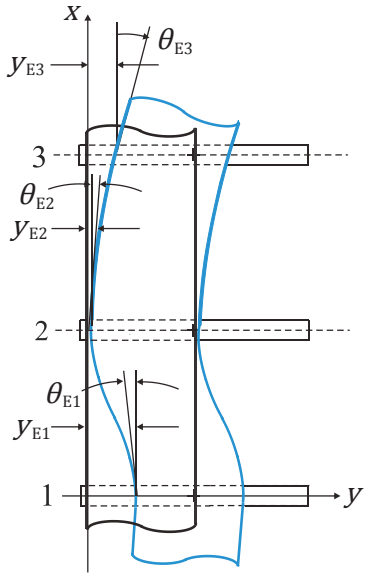

Figure 1: Three-roller system with input offset and input angle change at roller 1 (Brandenburg and Klemm, 2019, Figure 5.5)

2.1 Definition of the lateral register error

If a lateral web deflection $y_{E2}(t)$ is caused at roller 2 as a result of a disturbance at roller 1, then, since the synchronism of the printing units is maintained, and the longitudinal change in web elongation is negligibly small, the lateral register error (LRF) $Y_{y,E2}(t)$ is directly given by this web deflection. Thus, the definition equation is

$$Y_{y,E2}(t) = y_{E2}(t) \quad [1]$$

In the s-domain it reads

$$Y_{y,E2}(s) = y_{E2}(s) \quad [2]$$

To calculate the LRF, the time $t_{L,12}$ is important, which a point needs to travel the length L_{12}. As is known, this is the time constant

$$t_{L,12} = T_{12} = L_{12}/v \quad [3]$$

An important tool for the mathematical description of the lateral motion of the web is the block diagram of Figure 2, which was first developed in Brandenburg and Klemm (2019).

2.2 Register error at input displacement and input angle change

The input displacement y_{E1} is assumed to be a step function at the time $t = t_{p1}$, the printing time of printing unit 1 (DW 1). This means that there is a lateral register error which is transported with the web and reaches roller 2 after the run time T_{12}

$$Y_{y,E2}(t) = y_{E1}(t - T_{12}) \quad [4]$$

In the s-domain, this equation reads as follows

$$Y_{y,E2}(s) = e^{-T_{12}s} y_{E1}(s) \quad [5]$$

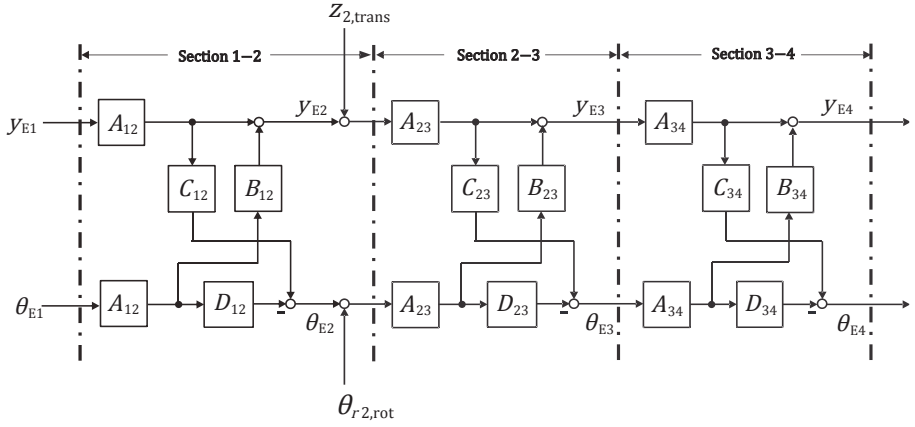

Figure 2: Block diagram of the lateral web motion at constant velocity according to Brandenburg and Klemm (2019, Figure 5.12)

However, the input displacement also triggers an immediate lateral transient $f^{(1)}[y_{E1}(t)]$, which leads to an additional LRF at roller 2. Then the total LRF at roller 2 is given by

$$Y_{y,E2}^{(1)}(t) = y_{E1}(t - T_{12}) + f^{(1)}[y_{E1}(t)] \quad [6]$$

In the s-domain this equation is

$$Y_{y,E2}^{(1)}(s) = e^{-T_{12}s} y_{E1}(s) + \phi^{(1)}[y_{E1}(s)] \quad [7]$$

Since the Bernoulli web obeys the block diagram of Figure 2, the following relationship is valid

$$\phi^{(1)}[y_{E1}(s)] = A_{12}(s) y_{E1}(s) \quad [8]$$

If a change of the input angle $\theta_{E1}(t)$ simultaneously occurs, this triggers a transient

$$Y_{y,E2}^{(2)}(s) = e^{-T_{12}s} \theta_{E1}(s) + \phi^{(2)}[\theta_{E1}(s)] \quad [9]$$

which is to be added to Equation [7]

$$Y_{y,E2}^{(1+2)}(s) = e^{-T_{12}s} y_{E1}(s) + \phi^{(1)}[y_{E1}(s)] + e^{-T_{12}s} \theta_{E1}(s) + \phi^{(2)}[\theta_{E1}(s)] \quad [10]$$

The result is

$$Y_{y,E2}^{(1+2)}(s) = \phi^{(1)}[y_{E1}(s)] + \phi^{(2)}[\theta_{E1}(s)] + [y_{E1}(s) + \theta_{E1}(s)] e^{-T_{12}s} \quad [11]$$

From the block diagram of Figure 2, *the complete lateral register error at constant web speed* then follows to be

$$Y_{y,E2}^{(1+2)}(s) = A_{12}(s) y_{E1}(s) + A_{12}(s) B_{12}(s) \theta_{E1}(s) + [y_{E1}(s) + \theta_{E1}(s)] e^{-T_{12}s} \quad [12]$$

This entire register error is simply called $Y_{y,E2}$

$$Y_{y,E2}(s) = A_{12}(s) y_{E1}(s) + A_{12}(s) B_{12}(s) \theta_{E1}(s) + [y_{E1}(s) + \theta_{E1}(s)] e^{-T_{12}s} \quad [13]$$

This Equation [13] reads in words: Both input variables, $y_{E1}(s)$ and/or $\theta_{E1}(s)$ immediately result in a lateral register error at roller 2 for $t > t_{p1}$. At the same time, however, they are also printed by printing unit 1 at the time $t = t_{p1}$, transported by the web and do not reach roller 2 until the transport time T_{12} has elapsed.

According to Brandenburg and Klemm (2019, section 5.2.6), the transfer functions $A_{12}(s)$ and $B_{12}(s)$ are generally given by

$$A_{i,i+1} = \frac{1}{\frac{T_{(i,i+1)}^2}{f_{B(i,i+1)}} s^2 + K_{CB(i,i+1)} T_{(i,i+1)} s + 1} \quad [14]$$

$$B_{(i,i+1)} = \frac{u_{(i,i+1)} - \sinh(u_{(i,i+1)})}{S_{(i,i+1)}} K_{CB(i,i+1)} L_{(i,i+1)} \quad [15]$$

and are specifically for $i = 1$ and $i + 1 = 2$ in system 1–2

$$A_{12} = \frac{1}{\frac{T_{12}^2}{f_{B12}} s^2 + K_{CB,12} T_{12} s + 1} \quad [16]$$

$$B_{12} = \frac{u_{12} - \sinh(u_{12})}{S_{12}} K_{CB,12} L_{12} \quad [17]$$

From Equation [17] it can be seen that B_{12} contains the factor L_{12} which provides dimensional correctness. It would have been more clever to use a function

$$B_{12}^* = \frac{B_{12}}{L_{12}} = \frac{u_{12} - \sinh(u_{12})}{S_{12}} K_{CB,12} \quad [18]$$

in order to make the dimensional correctness visible by the term $B_{12}^* L_{12}$. But Equation [13] is maintained in the above form because of earlier publications.

3. Lateral and longitudinal register error at variable web strain and web speed as well as at input changes

3.1 Lateral register error

In order to treat variable web velocities and web strain, the system equations have to be linearized. Since Equation [13] is a linear relation, it is also valid for small deflections from the steady state (marked by a tilde)

$$\tilde{Y}_{y,E2}(s) = A_{12}(s) \tilde{y}_{E1}(s) + A_{12}(s) B_{12}(s) \tilde{\theta}_{E1}(s) + [\tilde{y}_{E1}(s) + \theta_{E1}(s)] e^{-T_{12}s} \quad [19]$$

the time constant of the web can be assumed to be constant because of the only small changes in web velocity. That a steady state with stationary deflection and stationary angle exists is proved for the Bernoulli web using the equations of the two-mass system in Brandenburg and Klemm (2019, Equation [4.38]), for $y_0 = \hat{y}_0 = \hat{y}_{E1}$. The stationary deflection is

$$\lim_{t \to \infty} y_{E2}(t) = \lim_{s \to 0} y_{E2}(s) = \hat{y}_{E1} \quad [20]$$

From Brandenburg and Klemm (2019, Equations [4.61] and [4.65]) the stationary web angle is calculated to be

$$\lim_{t\to\infty} y_{E2}(t) = \lim_{s\to 0} y_{E2}(s) \qquad [21]$$
$$= \frac{u - \sin h(u)}{\sin h(u) - u\cos h(u)} K_{CB} L\hat{\theta}_{E1}$$
$$= \frac{u - \sin h(u)}{u[\cos h(u) - 1]} L\hat{\theta}_{E1}$$

Thus, the linearization is justified. Then the equations for further systems 2–3 and 3–4 read

$$\tilde{Y}_{y,E3}(s) = A_{23}(s)\tilde{y}_{E2}(s) + A_{23}(s)B_{23}(s)\tilde{\theta}_{E2}(s) \cdot \qquad [22]$$
$$+ [\tilde{y}_{E2}(s) + \tilde{\theta}_{E2}(s)]e^{-T_{23}s}$$

and

$$\tilde{Y}_{y,E4}(s) = A_{34}(s)\tilde{y}_{E3}(s) + A_{34}(s)B_{34}(s)\tilde{\theta}_{E3}(s) \qquad [23]$$
$$+ [\tilde{y}_{E3}(s) + \tilde{\theta}_{E3}(s)]e^{-T_{34}s}$$

3.2 Longitudinal and lateral register error due to input displacement

The question is now whether there is a relationship between lateral and longitudinal register error. For this purpose, Figure 3 is discussed.

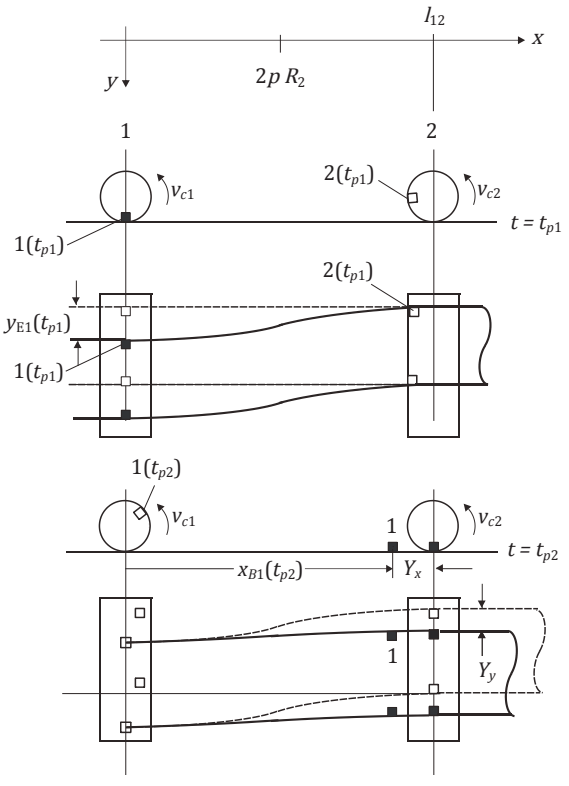

Figure 3: Part of three-roller system with input offset and input angle change at roller 1, from Brandenburg and Klemm (2019, Figure 5.5)

At the printing time $t = t_{p1}$, a step function of the input displacement $y_{E1}(t_{p1})$ is assumed. With this lateral register error (LRF), the first print unit DW 1 prints the point "1", symbolically written in the form $1(t_{p1})$ in Figure 3. In the top view of Figure 3, two points at the edge of the web are chosen: A black point means that this one will be printed, a white one means that this one will not be printed. It is now arbitrarily assumed that point 1 at the printing time $t = t_{p2} = t_{p1} + T_{12}$ of DW 2, does not exactly reach the assigned point of DW 2, but lies somewhat behind or in front of it (as is drawn in Figure 3). So at the time $t = T_{12}$ there is also a longitudinal register error $Y_{x,E2}$. Now, however, the described lateral dynamic process was triggered at the same time by the input displacement, which at the time $t_{p2} = t_{p1} + T_{12}$ causes the lateral register error $Y_{y,E2}$. Thus, the longitudinal and lateral register errors are coupled with each other at any time. Of course, this does not mean that a lateral register error will cause a longitudinal one. A longitudinal register error can be added at some time during an "ongoing" lateral dynamic process.

3.3 Mathematical formulations

The linearized *longitudinal* register error obeys in the *s*-domain the long-known relation

$$\tilde{Y}_{x,E2}(s) = \frac{\bar{v}}{s}[-\tilde{\varepsilon}_{12}(s) + e^{-T_{12}s}\tilde{\varepsilon}_{01}(s)] \qquad [24]$$

In Equation [24], the first term in the square brackets describes all points (1) that are already located in the web section 1–2 when the transient starts, while the term $e^{-T_{12}s}\tilde{\varepsilon}_{01}(s)$ describes those points (2) that enter at DW 1 for $t \geq 0$ and arrive at DW 2 after the transport time T_{12} has elapsed. For the linearized lateral register error $\tilde{Y}_{y,E2}$ the above given Equation [19] is valid.

In order to mathematically describe the coupling of longitudinal and lateral register error, the following assumptions are made:

- The longitudinal web deflection, which occurs in *x*-direction, and the lateral web deflection, which occurs in *y*-direction, are treated separately.
- The lateral movement caused by the input displacement does not cause any strain in the *x*-direction.

If both simultaneously occurring register errors were present in the time domain, then both expressions would have to be added in the entire time domain for the same point in time, respectively. The corresponding mathematical formulation is:

Given $Y_{x,12} = f(t)$ and $Y_{y,12}(t)$. The inverse function of $Y_{x,12}$ is: $t = g(Y_{x,12})$. This time is inserted into $Y_{y,12}(t)$. Then the total function, i.e. the total register error, follows to be

$$Y_{y,12}(t) = Y_{y,12}\big[g\big(Y_{x,12}(t)\big)\big] \qquad [25]$$

By this transformation the same time was determined for both parts. This requires that the functions can be reversed analytically. When assessing the significance of this number, it must be taken into account that both errors lie in the same plane, namely the web plane, but are perpendicular to each other.

In the *s*-domain, the function pair of Equation [19]

$$\tilde{Y}_{y,\mathrm{E2}}(s) = A_{12}(s)\tilde{y}_{\mathrm{E1}}(s) + A_{12}(s)B_{12}(s)\tilde{\theta}_{\mathrm{E1}}(s) + [\tilde{y}_{\mathrm{E1}}(s) + \theta_{\mathrm{E1}}(s)]e^{-T_{12}s} \quad [26]$$

and Equation [24]

$$\tilde{Y}_{x,\mathrm{E2}}(s) = \frac{\tilde{v}}{s}[-\tilde{\varepsilon}_{12}(s) + e^{-T_{12}s}\tilde{\varepsilon}_{01}(s)] \quad [27]$$

describes both register errors in parameter representation. Parameter is the operator *s*.

In Figure 4, the block diagram is drawn, which illustrates the interaction of lateral and longitudinal register error according to Equations [29] and [28] for a three-roller system. The upper chain shows the lateral register error $\tilde{Y}_{y,\mathrm{E}i}$, the lower chain the longitudinal register error $\tilde{Y}_{x,\mathrm{E}i}$. It can be seen that both register errors are linked to the mass flow chain. The name "multi-layer model" is introduced for this system plan.

The upper system for lateral motion and the lower one for longitudinal motion can be excited and simulated completely independently of each other, i.e. for any time points $\tilde{y}_{\mathrm{E1}}(t = t_1), \tilde{\theta}_{\mathrm{E1}}(t = t_2)$ and $T^*_{01}(t = t_3)$. However, to illustrate the two-dimensional register errors $\tilde{Y}_{(Si,i+1)}$, one time point $t_1 = t_2 = t_3$ has to be chosen. Since both register errors are perpendicular to each other, it is proposed to represent the quantities $\tilde{Y}_{x,\mathrm{E}i}$ and $\tilde{Y}_{y,\mathrm{E}i}$ as components of vectors

$$\vec{\tilde{Y}}_{x,\mathrm{E}i} = \tilde{Y}_{x,\mathrm{E}i}\vec{e}_x \quad [28]$$

and

$$\vec{\tilde{Y}}_{y,\mathrm{E}i} = \tilde{Y}_{y,\mathrm{E}i}\vec{e}_y \quad [29]$$

Where $\vec{e}_x$ and $\vec{e}_y$ are the unit vectors in *x*- and *y*-directions. The sum vector, i.e. the vector of the total register error, is then given by

$$\vec{\tilde{Y}}_{s,\mathrm{E}i} = \vec{\tilde{Y}}_{x,\mathrm{E}i} + \vec{\tilde{Y}}_{y,\mathrm{E}i} = \tilde{Y}_{x,\mathrm{E}i}\vec{e}_x + \tilde{Y}_{y,\mathrm{E}i}\vec{e}_y \quad [30]$$

During a dynamic process, this vector changes its magnitude and angle while the web is running.

In the block diagram of Figure 4, the following three variables appear as independent input variables: the input displacement and the input angle of the web as well as

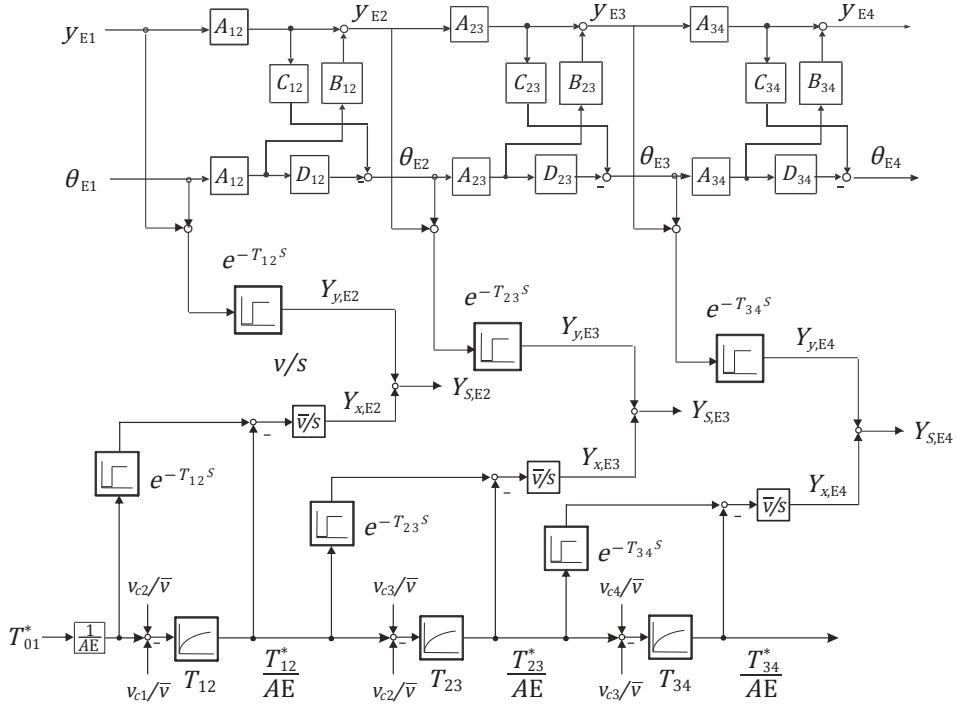

Figure 4: Total system diagram: interaction of lateral and longitudinal register errors (multi-layer model); all variables are small deviations from steady state

the change in tensile force at the input of the mass flow chain. They are defined to be "main input variables", because they can excite all three layers. The circumferential speeds of the rollers, however, are assigned to the corresponding time lags of the mass flow chain.

Thus, this multi-layer model, together with corresponding simulations, allows quantitative predictions about the dynamics of all system variables. The retroactive effect of forces on lateral web motion and the lateral register errors was neglected. If this simplification is admissible must be justified in the specific case (Brandenburg and Klemm, 2017).

4. Conclusion

The multi-layer model in Figure 4 represents the overall system of lateral and longitudinal register errors and the mass flow chain. This study clearly shows the interaction of important influencing variables that make visible the behavior of the information printed on the web and the associated errors. From the point of view of control technology, this system representation offers the possibility of using simulations to test and quantitatively assess the control performance and in particular the behavior in relation to numerous disturbances.

Acknowledgment

I want to express my sincere thanks to Dr. Andreas Klemm for fruitful discussions and carrying out formatting guidelines.

List of symbols

If x is a variable, $\bar{x}$ denotes the steady state and $\tilde{x}$ a small deviation of this variable from the steady state. Some of the chosen formula symbols follow directly from the context and explain themselves.

A_{12}	Transfer function according to Equations [14] and [16]
B_{12}	Transfer function according to Equations [15] and [17]
e	Base of the natural logarithm
$\vec{e}_x$	Unit vector in x-direction (longitudinal direction), Eq. [28]
$\vec{e}_y$	Unit vector in y-direction (lateral direction), Equation [29]
$g(Y_{x,12}(t))$	Inverse function of $Y_{x,12}(t)$ according to Equation [25]
s	Operator of Laplace transform
T_{12}	Time constant of web section 1–2 according to Equation [3]
$T_{(i,i+1)}$	Time constant of section $i, i+1$
$T^*_{(i,i+1)}$	Web force of section $i, i+1$
v	Speed of the web in x-direction
v_{ci}	Circumferential speed of a roller (= substitute quantity for the transport speed of a printing unit acting on the web i)
$\bar{v}$	Average transport velocity according to Equation [24]
$\vec{\tilde{Y}}_{x,\mathrm{E}i}$	Longitudinal register error in vector notation, Equations [28] and [29]
$\vec{\tilde{Y}}_{y,\mathrm{E}i}$	Lateral register error in vector notation, Equation [29]
$Y_{S,\mathrm{E}i}$	Sum of lateral and longitudinal register error (see Equation [30] and Figure 4)
$Y_{x,\mathrm{E}i}$	Longitudinal register error at the input roller i according to Equation [24]
$Y_{y,\mathrm{E}i}$	Lateral register error at the input roller i according to Equation [1]
$y_{\mathrm{E}i}$	Input displacement at roller i (cf. Figure 1)
$\varepsilon_{(i,i+1)}$	Strain in the free web section $i, i+1$
$\theta_{\mathrm{E}i}$	Input angle at roller i (cf. Figure 1)

References

Brandenburg, G., 1976a. *Verallgemeinertes Prozeßmodell für Fertigungsanlagen mit durchlaufenden Bahnen und Anwendung auf Antrieb und Registerregelung bei Rotationsdruckmaschinen*. Habilitationsschrift. Technische Universität München.

Brandenburg, G., 1976b. Verallgemeinertes Prozeßmodell für Fertigungsanlagen mit durchlaufenden Bahnen und Anwendung auf Antrieb und Registerregelung bei Rotationsdruckmaschinen. *Fortschrittberichte der VDI Zeitschriften*, *Reihe 1, Konstruktionstechnik, Maschinenelemente*, 46.

Brandenburg, G., 1976c. New mathematical models for web tension and register error. In: *Proceedings of 3rd International IFAC Conference on Instrumentation and Automation in the Paper, Rubber and Plastics Industries*, PRP 3. Brussels, Belgium, 24–26 May 1976. Leiden: Spruyt, Van Mantgern & De Does, pp. 411–438.

Brandenburg, G., 2000. Dynamisches Verhalten von Dublier- und Registerfehlern bei Rollenoffset Druckmaschinen. In: *Tagungsband SPS/IPC/DRIVES 2000*. Nurnberg, Germany, 28–30 November 2000. Heidelberg: Hüthig-Verlag, pp. 698–715.

Brandenburg, G., 2011. Advanced process models and control strategies for rotary printing presses. In: *Proceedings of the 11th International Conference on Web Handling*. Stillwater, OK, USA, 12–15 June 2011. Stillwater: Oklahoma State University.

Brandenburg, G., 2015. Fortgeschrittene Prozessmodelle und Regelungsverfahren für Rollen-Rotationsdruckmaschinen. In: D. Schröder, ed. *Elektrische Antriebe – Regelung von Antriebssystemen.* 4th ed. Berlin, Germany: Springer Vieweg, pp. 1472–1539.

Brandenburg, G., Geissenberger, S., Kink, C., Schall, N.-H. and Schramm, M., 1999. Multimotor electronic line shafts for rotary offset printing presses: a revolution in printing machine techniques. *IEEE/ASME Transactions on Mechatronics*, 4(1), pp. 25–31. https://doi.org/10.1109/3516.752081.

Brandenburg, G. and Klemm, A., 2017. Lateralverhalten kontinuierlicher elastischer Bahnen, Balkenmodell von Shelton und Erweiterungen. In: U. Fügman, ed. *Modellbildung und Zustandsüberwachung der Bahnführung: Proceedings zum 13. Bahnlaufseminar 2016.* Chemnitz, Germany, 19–20 September 2016. Berlin, Germany: VWF Verlag, pp. 35–104.

Brandenburg, G. and Klemm, A., 2019. Lateralverhalten elastischer Bahnen bei Berücksichtigung des Schubeinflusses. In: U. Fügman, ed. *Modellbildung und Simulation: Proceedings zum 14. Bahnlaufseminar 2018.* Chemnitz, Germany, 18–19 September 2018. Berlin, Germany VWF Verlag für Wissenschaft und Forschung, pp. 53–150.

Brandenburg, G. and Tröndle, H.-P., 1976a. Dynamik des Längsregisters bei Rollenrotationsdruckmaschinen: Teil 1. *Siemens Forschungs- und Entwicklungsberichte,* 5(1), pp. 17–20.

Brandenburg, G. and Tröndle, H.-P., 1976b. Dynamik des Längsregisters bei Rollenrotationsdruckmaschinen: Teil 2. *Siemens Forschungs- und Entwicklungsberichte,* 5(2), pp. 65–71.

Kang, H., 2010. *Two-dimensional register modeling and control for multi-layer roll-to-roll printing systems*. Ph.D. thesis. Konkuk University Seoul, Korea.

Kang, H., Lee, C. and Shin, K., 2011. Two-dimensional register modeling and control in multi-layer roll-to-roll e-printing systems. *IFAC Proceedings Volumes*, 44(1), pp. 6763–6770. https://doi.org/10.3182/20110828-6-IT-1002.03667.

Tröndle, H.-P., 1973. *Zum dynamischen Verhalten transportierter elastischer und visko-elastischer Stoffbahnen zwischen aufeinanderfolgenden Klemmstellen*. Dr.-Ing. Dissertation. Technische Universität München.